Effect of Joint Orientations on Blast Induced Damage in Gneiss Rock Mass Subjected to Repeated Blast Vibrations

M. Ramulu[1] and T.G. Sitharam[2]

Abstract

Blasting produces seismic waves similar to those produced by earthquakes, but with relatively high frequency and low amplitude and the degree of structural damage depends on the total energy of explosion, distance from the source, and the character of the medium. This paper deals with the research work carried out on the effect of repeated blast vibrations at Lohari Nag Pala Hydroelectric Power Construction Project in India. Multiple rounds of blasts were conducted at the penstock tunnels and at the excavation site for powerhouse foundation. The damage caused by blast induced vibrations can be categorized into two types: i) near-field damage due to high frequency vibrations when the blast is occurring in the close proximity and ii) far-field damage due to low frequency vibrations when the blast is occurring relatively farther distances. The near-field damage was assessed by Holmberg-Persson model by means of monitoring ground vibrations and by borehole camera inspection surveys. The far-field damage was assessed by measuring deformations of borehole extensometers and by borehole camera inspection surveys. Peak particle velocities (V_{max}) generated by blast rounds were recorded by installing triaxial geophones near the borehole extensometers and borehole camera inspection holes. Damage assessment instrumentation was carried out at both the sides of penstock tunnel wall as another objective of the study was to compare the extent of rock mass damage with different joint orientations. The blast induced damage was monitored by borehole extensometers, borehole camera inspection surveys and triaxial geophones installed at three test sites of different joint orientations at the Main Access Tunnel of power house. The study reveals that there was extra damage of 60% exclusively due to repeated blast vibrations. The results of the study indicate that repeated dynamic loading, resulted in damage even at 33% of the conventional damage threshold vibrations (V_c) in case of favorable joint orientations and 23% of V_c in case of unfavorable joints. The paper concludes in quantification of effect of repeated blast loading and the orientation of joints on the extension of damage zone in jointed rock mass of underground excavations.

Keywords: Tunnelling, Repeated blasting, Rock mass damage, Peak particle velocity.

Introduction

Blasting produces seismic waves similar to those produced by earthquakes, but with relatively high frequency and low amplitude and the degree of structural damage depends on the total energy of explosion, distance from the source, and the character of the medium. Blast induced damage weakens a rock mass, potentially leading to stability problems in the underground excavations. The blast damage problem is more severe and vulnerable for the jointed rock mass in underground excavations (Singh and Xavier 2005). Unfortunately, there are no specific safety guidelines available for the blasted tunnels with regards to the threshold limits of vibrations caused by repeated blasting activity in the close proximity. Studies on

[1]Scientist, Central Institute of Mining & Fuel Research, Regional Centre, Nagpur-440006, India.
Tel:+91-712-2510604, Fax: :+91-712-2510311, more.ramulu@gmail.com
[2]Professor, Department of Civil Engineering, Indian Institute of Science, Bangalore, India,
sitharam@civil.iisc.ernet.in

blast induced damage on underground openings are well documented by many researchers globally (Langefors and Kihlstrom, 1963, Hendron 1977, Holmberg 1993, Singh 1993, and Chakraborty et al., 1998). Joint orientation with respect to perimeter line of underground opening is one of the influencing parameters of blast induced damage (Cunningham & Goetzsche, 1996). Singh and Xavier (2005) observed largest overbreak for the joint orientations of 45^0 and minimum overbreak for parallel and perpendicular joint orientations and similar results were also obtained by Lewandowski et al. (1996). The rock mass damage problem will be manifold if the blast loading is applied for repeated number of times, in contrast to the conventional single episode blast loading. Repeated blast loading causes progressive accumulation of damage in joints, which may lead to achievement of residual strength state in joints, with resultant large displacement at the joint surface (Brady 1990). The effect of repeated blast loading on jointed rock mass was qualitatively studied by many researchers globally (Atchison and Pugliese, 1964; Brady, 1990; Law et al., 2001; Villaescusa et al., 2004). Brown and Hudson (1974) states that rock mass damage by blast loading is predominantly due to joint motion, which is consistent with the experimental observation that joints decrease in shear strength under cyclic shear loading. Model studies of excavations in jointed rock under cyclic loading by Barton and Hansteen (1979) confirmed that excavation failure occurred by accumulation of shear displacements at joints. On the basis of these findings, St. John and Zahrah (1987) stated that, under dynamic loading, it is the number of excursions of joint motion into the plastic range that determines damage to an excavation. Wagner (1984) provided an indication of the general inadequacy of dynamic design based on peak particle velocity (V_{max}) of single blast round.

Although far-field damage is not a severe problem at the excavation sites where the blasting faces moves away and vibration gets attenuated substantially, it was observed, by the authors, as an acute problem when the rock mass is subjected to repeated vibrations due to multiple excavations in the vicinity. In this paper, it was aimed at the prediction and assessment of blast induced damage and deterioration due to repeated vibrations in adjacent tunnel blasting, which is at a distance of 10-15m on either side, and the open-cut blasting for excavation of power house foundation.

Site Description

General

The Lohari Nag Pala Hydroelectric Power Project (LNPHPP) of 600MW capacity is located on the right bank of Bhagirathi River (Fig. 1) in the Central Crystallines of Higher Himalayan Zone in Uttarkashi District of Uttarakhand State at about 230 km from Rishikesh on National Highway No.108. The project consists of 73.40 m long barrage across river Bhagirathi and major underground structures under excavation include 14 km long 6m diameter (horse-shoe) head race tunnel (HRT), 155m (L) X 22m (W) X 47m (H) size power house and 350m long tail race tunnel (TRT). The water from the river will be transferred to the power house through the HRT and discharged back in to the river Bhagirathi through the 7.5 m diameter (horse-shoe shape) TRT. The Power house is proposed to house four power generation units of 150 MW each. The construction of HRT will be done from three numbers of intermediate construction adits apart from inlet and outlet ends, which will facilitate the excavation from eight faces. Other structures of power house complex (Fig. 2) are Main Access Tunnel (MAT) of 8m diameter (D-shape), a Cable & Ventilation Tunnel (CVT) of 6m diameter (D-shape), TRT adit, etc. As there were repeated blast loadings on the underground openings, the experimentation was designed to determine the effect of repeated vibrations on rock mass damage, on the basis of previous experience of the authors (Ramulu, 2009). The damage assessment was carried out at both the side

walls of the tunnel as the joint orientation with respect to tunnel perimeter line was making acute angle at the left side and obtuse angle at the right side of the tunnel. The damage assessment was also carried out at crown rock mass of the tunnel where the joint orientation was making nearly 180^0 angle with respect to tunnel perimeter line. The objective of damage assessment at three different locations is to know the effect of joint orientation with respect to the perimeter line of the tunnel. The tunnel profile where the experimentation was carried out is shown in Fig. 3.

Geological and geotechnical information of experimental site

The area encompassing LNPHPP in the Uttarkahsi region of Uttrakhand Himalayas is made up of two main tectonic units, viz. the Central Crystallines and the Lesser Himalayan formations. The slab of the Central Crystallines are thrusted over the quartzite and volcanic of Berinag Formation of the Lesser Himalayas or rock belonging to Garhwal Group along the Main Central Thrust (MCT). The Garhwal Group towards north is followed by the Central Crystallines which have been divided into three zones i.e. Upper Crystallines, Middle Crystallines and Lower Crystallines.

The main rock type of powerhouse complex is schistose gneiss and augen gneiss with abundance of mica and geotechnically the rock mass falls in "Fair Category" with three

Fig. 1: Location of the LNPHPP site on Bhagirathi River, Uttaranchal, India

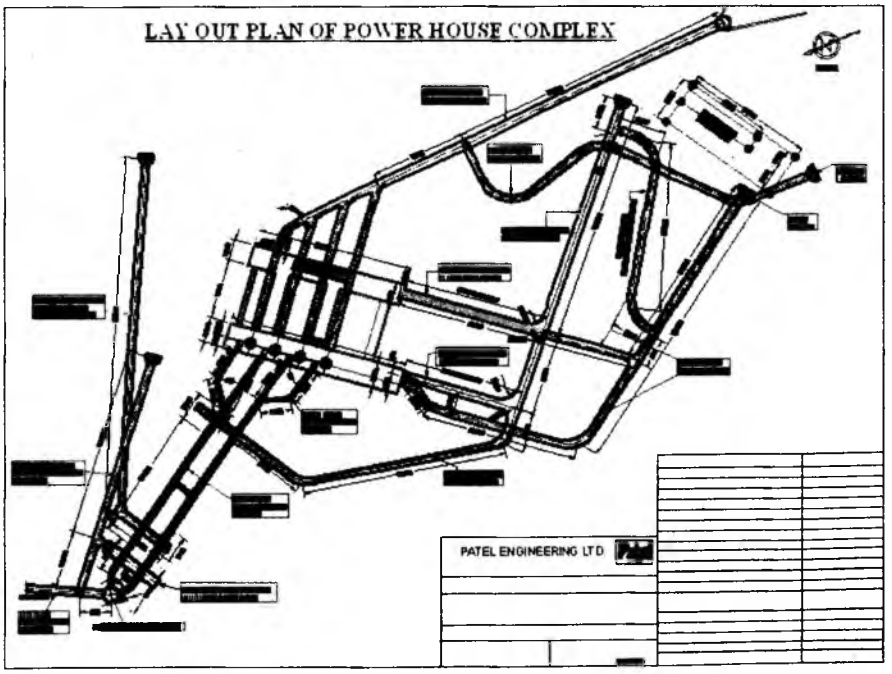

Fig. 2: Plan view of the power house complex, LNPHPP

(a) Tunnel portal

(b) Excavated tunnel profile

Fig. 3: Experimentation tunnel with varying joint orientations at both left and right-sides

prominent joint sets. Two joint sets intersect at right angle, which makes wedge continuously. Some weak zone/clay filling, altered rock, sheared rock mass and excessive flow of water at places makes the rock poor. Mostly, the regional trend of foliation is perpendicular to the tunnel alignment, another joint which is intersecting the foliation at right angle and creates wedge on roof. The strike of the foliation is going through along the tunnel alignment which is geologically not favorable because of probabilities of plane failure and wedge failure in presence of heavy joint planes. The detailed geological information is given in the Table 1. Core samples were collected from both the monitoring locations by underground coring machine. Engineering properties like Rock Quality Designation (RQD) compressive strength, tensile strength, density and compressional wave velocity (Vp) were determined from the core samples. In-situ compressive strengths were also determined by using Schmidt rebound hammer. The average intact rock properties of the Schistose/Augan gneiss at two different experimental locations are given in Table 2.

Table 1. General geological information

Location	Crown to Spring level (Both Sides)	Below Spring level (Left-side)	Below Spring level (Right-side)
Rock type	Schistose/Augen gneiss with alternative bands of mica & quartz	Mica schist with alternative bands of quartz	Schistose/Augan gneiss with bands of mica and quartz
Critical joint angle	$50^0/52^0$, $210^0/50^0$	$095^0/55^0$, $175^0/45^0$	$095^0/55^0$, $175^0/45^0$
Seepage	Moderate	Continuous	Occasional
Wedge portion	Crown	None	Walls
Spacing	6-20cm, 20-60cm	6-20cm, 20-60cm	<6cm, 6-20cm
Opening	0.25-2.5mm	0.25-2.5mm	0.25-2.5mm
Joint Alteration	Altered joint, highly stained	Moderately altered joint walls	Moderately altered joint walls
Rock Strength	Weak-Medium strong (25-50MPa)	Weak-Medium strong (25-50MPa)	Weak (5-25MPa)
Nos. of Joint Sets	Three joint sets + Random	Three joint sets + Random	Three joint sets + Random
Degree of Weathering	Slightly Weathered Rock	Moderately to Highly Weathered	Moderately Weathered
Water Inflow	Dripping (Low)	Damp	Seepage at places
Rock mass Quality (Q)	1.53-3.04 Poor rock	0.86-1.14, Poor rock	1.15-3.04, Poor rock

Table 2: Average intact rock properties of the Schistose/Augan gneiss

Location	Rock type	Mass Density, kg/m^3	Tensile strength, (MPa)	Young's modulus, (GPa)	P-wave velocity (m/s)
Right-side wall (Joint rientation=150^0)	Schistose/Augan gneiss with acute joint orientation	2450	3.5	21.5	2958
Left-side wall (Joint orientation=30^0)	Schistose/Augan gneiss with obtuse joint orientation	2445	3.1	19.25	2610

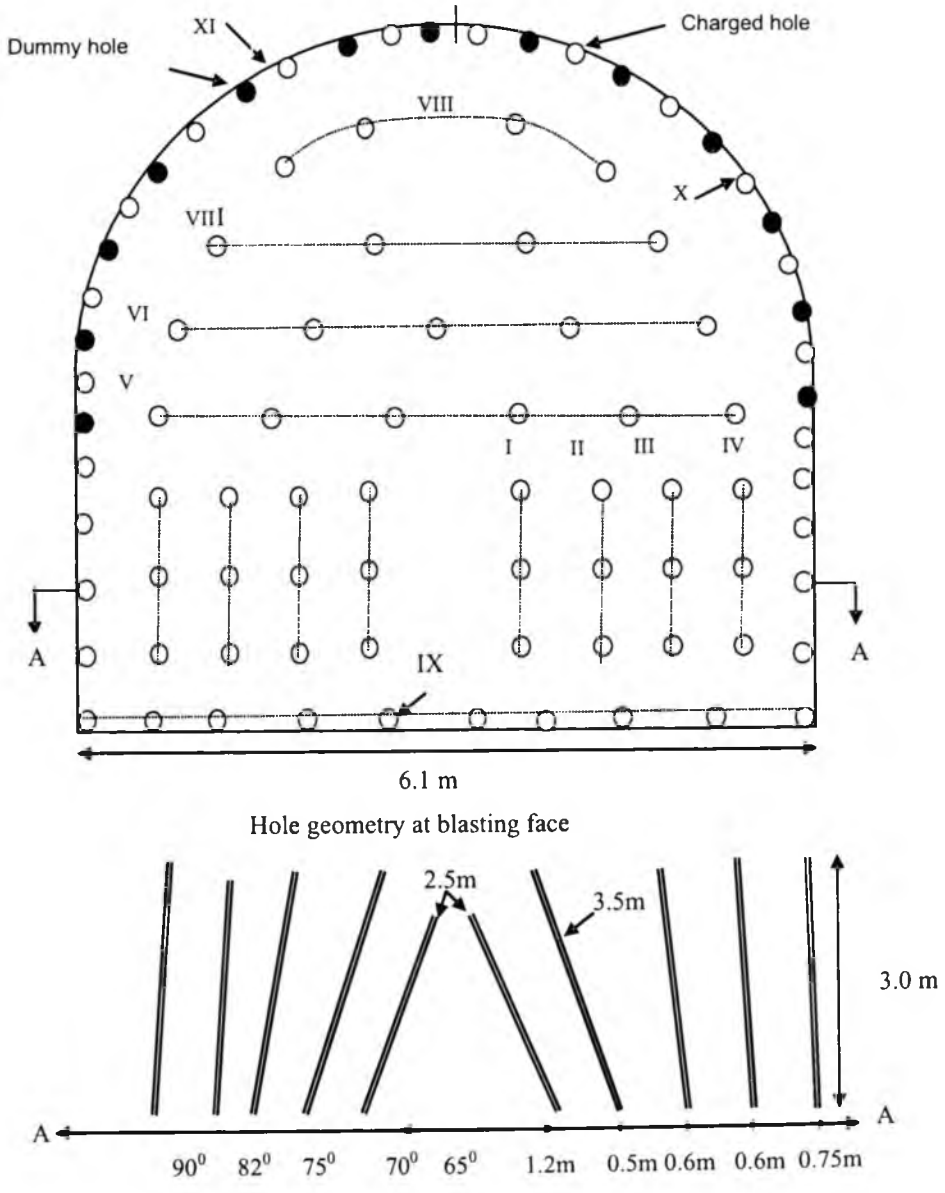

(The numbers in Roman letters denote delay numbers), Sectional view of blast holes (A-A)

Fig. 4: Blast design at power house complex, LNPHPP

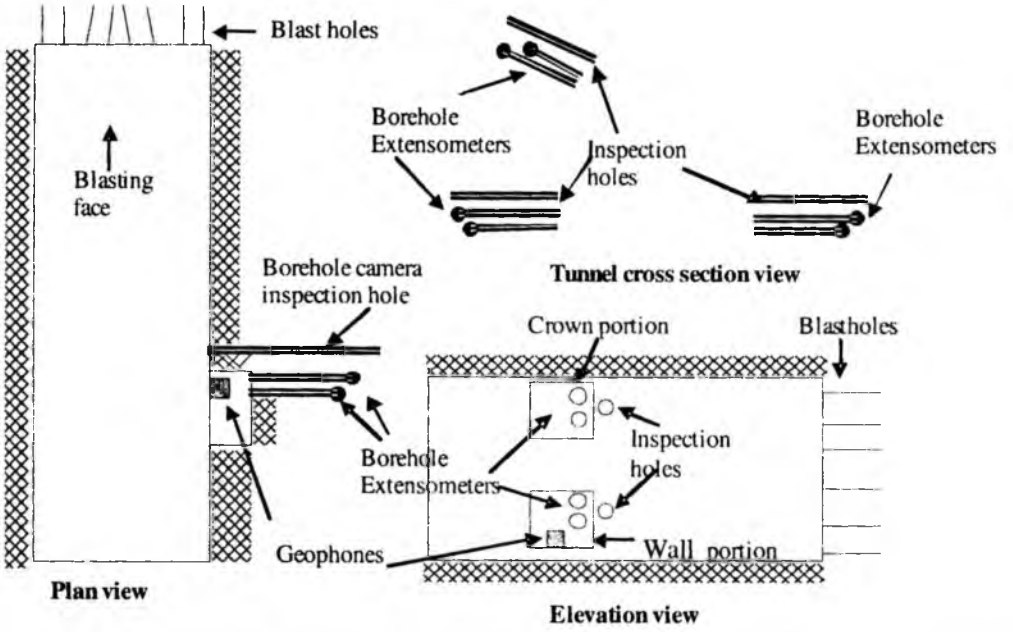

Fig. 5: Schematic installation locations of geophones, borehole extensometers and borehole camera inspection holes

Details of the Blasting and Instrumentation

The tunnel was excavated with heading and benching simultaneously by using drilling and blasting method. Rocket boomer was used for drilling of blast holes of 45mm diameter. Wedge cut blasting pattern was adopted with a maximum hole depth of 3.5m for the tunnels of 32m^2 area of cross section. The blast pattern practiced for the full face tunnel blasting at powerhouse complex is shown in Figure 4. The specific charge was varied depending on the static and dynamic properties of rock. The explosive used was cartridge emulsion with 80% strength. The in-hole velocity of detonation (VOD) of the explosive was determined as 3000-3100 m/s by using VOD monitoring instrument called SuperTrap (M/s MREL Inc., Canada). Long delay detonators from 1 to 10 were used to fire various rows in different delays. The maximum charge per delay used in the blast round was 32 kg in the bottom holes and total charge per round was 169kg. Total number of holes used were 87, which include 13 dummy holes at the Crown periphery of the tunnel line. The specific charge used for Schistose/ Augen gneiss was 1.75 kg/m^3. The progress per round with this blast pattern was observed as 2.5 to 2.75m out of 3m effective depth of blast round.

Instrumentation carried out in this study include, triaxial geophones for vibration monitoring, borehole camera survey for observing crack extension, loosening of joints and borehole extensometers for measurement of plastic deformations. It has become common practice, recently, to use peak particle velocity (V_{max}) as an indicator of the potential for rock mass damage, as the V_{max} is directly proportional to the dynamic strain (Jaeger & Cook, 1979). Numerous authors used V_{max} as criteria for blast damage in rock mass (Langefors and Kihlstrom, 1963; Kutter and Fairhurst, 1971; Holmberg and Persson, 1978; Holmberg and Persson, 1980; Oriard, 1982; Singh, 1993; Yu and Vongpaisal, 1996; Villaescusa et al., 2004). Application of borehole extensometers for blast damage inspections was reported by many authors globally (Niklasson, 1985; Stacey et al., 1990; Kim, et al., 1990; Villaescusa et al., 2004). Application of borehole camera for blast damage

inspections was reported by many authors globally (Niklasson, 1985; Beyer and Jacobs, 1986; Stacey et al., 1990; Rocque et al., 1992; Singh, 1993; Andrieux et al., 1994; Doucet et al., 1996; Liu et al., 1998). A room of 0.5 m^3 inside the wall of MAT was made for installation of geophones to capture the blast vibrations from the surrounding excavations and for the installation of borehole extensometers. The damage monitoring stations were located at the Chainage of 45m inside the MAT, which was exposed to the vibrations from face blasting of MAT, CVT as well as TRT adit. A typical damage monitoring set-up at the tunnel wall is shown in Fig. 5, where the geophones, borehole extensometers and borehole camera survey holes are shown. The location of borehole extensometers and geophones and blasting location is schematically shown in Fig. 6. The installation of borehole extensometer and geophones are shown in Fig. 7.

Experimentation on the Effect of Repeated Blast Loading

Near-field blast damage assessment

The near-field damage to the rock mass at the experimental station occurred due to the production blast rounds conducted within the tunnel. The near-field damage was assessed by borehole camera survey. An initial pre-blasting survey was performed in each hole to take pictures of pre-existing structural features for comparison with post blast surveys. A total of two borehole camera surveys were taken, one each at right side and left side tunnel walls. All the pictures were sorted out first by editing and matching the same images before and after each blast. Consequently, the pictures, which showed differences in fracture existence, were identified by their position coordinates. The images of inspection holes captured by borehole camera clearly indicated that the near-field damage due to production blasts extended up to 1.59m, 1.74m, and 1.53m at Left-side, Right-side and Crown rock mass, respectively.

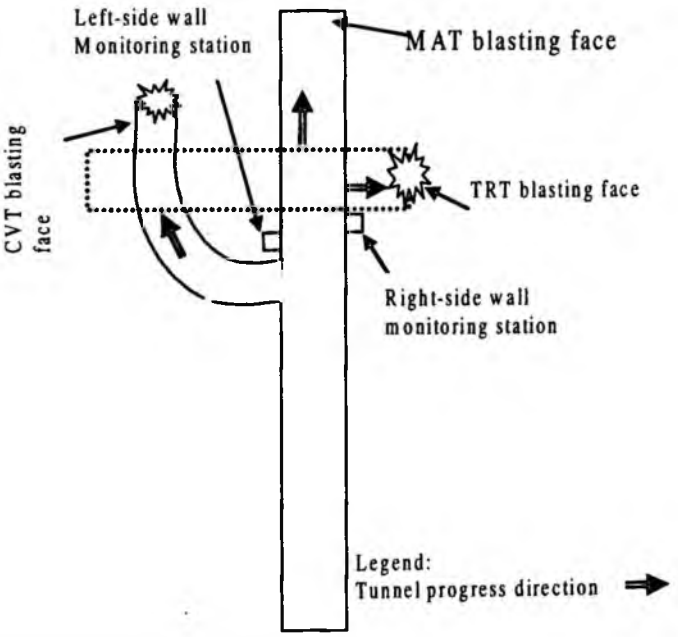

Fig. 6: Schematic view of vibration and damage monitoring stations with respect to blasting location

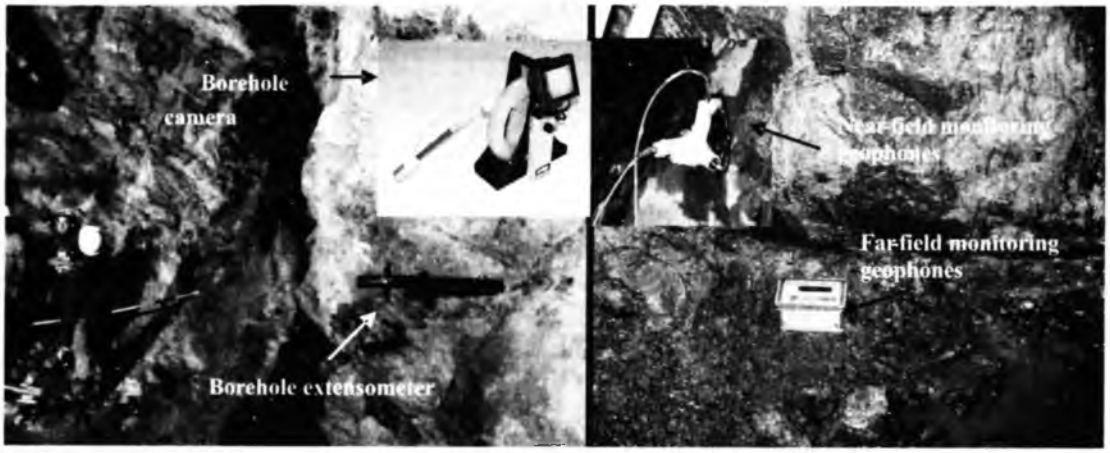

(i) (ii)

Fig. 7: The installation of (i) borehole extensometer and (ii) geophones

Far-field blast damage due to repeated vibrations

The multiple rounds of blasting activity was carried out for the power house room excavation at the downstream side of the penstock tunnels, which was in the close proximity of the tail end of penstock tunnel, where the monitoring instruments were installed. Far-field rock mass damage observations were carried out by using borehole camera and by borehole extensometer. In order to correlate the far field damage with the vibrations, the V_{max} levels were recorded for every blast round uptill the vibration intensity attenuated to about 45mm/s. All the damage observation systems were monitored for 60 rounds of blasts at all the three monitoring locations of MAT i.e. right-side wall, left-side wall and crown rock. As the blast site is moving away from the monitoring point the vibration intensity, obviously, reduced gradually below critical peak particle velocity. The effect of these reduced vibration levels with the repeated number of exposures on the extent of further damage was studied thoroughly by all the three instruments. The blast damage assessment at left-side and right-side wall of the MAT is discussed in the following sections.

(The numbers in Roman letters denote delay numbers)

Damage assessment at rock mass with acute angle joint orientation (30^0-45^0)

Peak particle velocities versus no. of occurrences of dynamic loading at gneiss rock mass with acute angle joint orientation is shown in Fig. 8. The vibration intensity range from 40 to 1753 mm/s at the monitoring location. The displacements of extensometer rods of 3 and 4m depth at the left-side tunnel wall were proportional to the V_{max} for few near-field blast rounds of MAT face blasts, where the V_{max} is above V_{cr} (Fig. 9). There was no considerable change in the extensometer readings of both 3 and 4m rods for all the V_{max} levels below V_{cr} (353mm/s) for the MAT and CVT face blasts. After 40 blast rounds, the displacements were again observed for TRT face blasts, even at the vibration levels 233.6 mm/s, which is below the V_{cr}. There were no displacements observed below the V_{max} level of 116mm/s. This effect gives an inference that the damage zone was below 3m from the tunnel perimeter. The exact depth of damage zone inside the tunnel walls could not be found with extensometers. Therefore, borehole camera observations were used for

determination of exact depth of damage as well as extent of crack network and fracture frequency. As the range of damage extension was already assessed by means of extensometer, the inspection of exact extension of damage by borehole camera had become much easier. Images were captured by an interval of 5cm, within the range of probable damage extension for precise inspection of rock mass damage. The images of borehole sections which contain the interface of intact and disturbed rock mass of tunnel wall are shown in Fig. 10. The damage depth measured by the borehole camera inspection survey at the left-side wall with acute joint orientation was 2.70m.

Damage assessment at rock mass with obtuse angle joint orientation (150-180^0)

Peak particle velocities versus no. of occurrences of dynamic loading at right-side of the tunnel are shown in Fig. 11. The vibration intensity recorded at the monitoring location ranged from 42 to 1644 mm/s. The displacements indicated by the extensometer rod of 3m depth at the right-side wall were proportional to the V_{max} for few blast rounds at the MAT whose V_{max} were above V_{cr} (427mm/s), as shown in Fig. 12. After 16 blast rounds, it was observed that the displacements suddenly dropped to negligible levels even though the V_{max} recorded was above V_{cr}. This effect gives an inference that the damage zone reached the anchor point of the 3.0m extensometer rod after few close

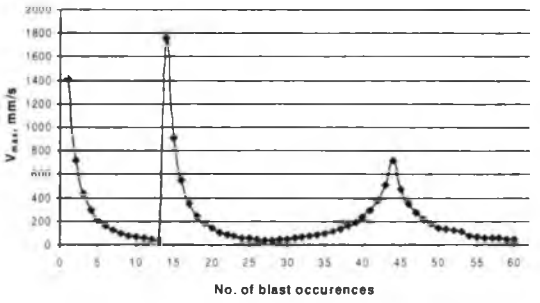

Fig. 8. Peak particle velocities versus no. of dynamic loading cycles for gneiss rock mass with acute joint orientation

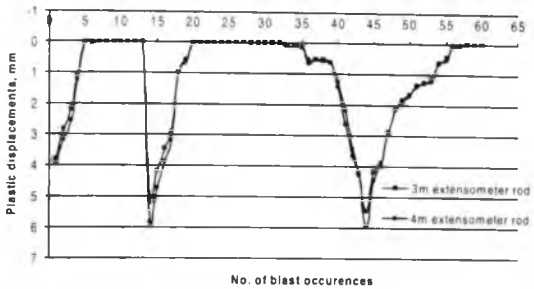

Fig. 9: Plastic deformations of extensometer rods in gneiss rock mass with acute joint orientation

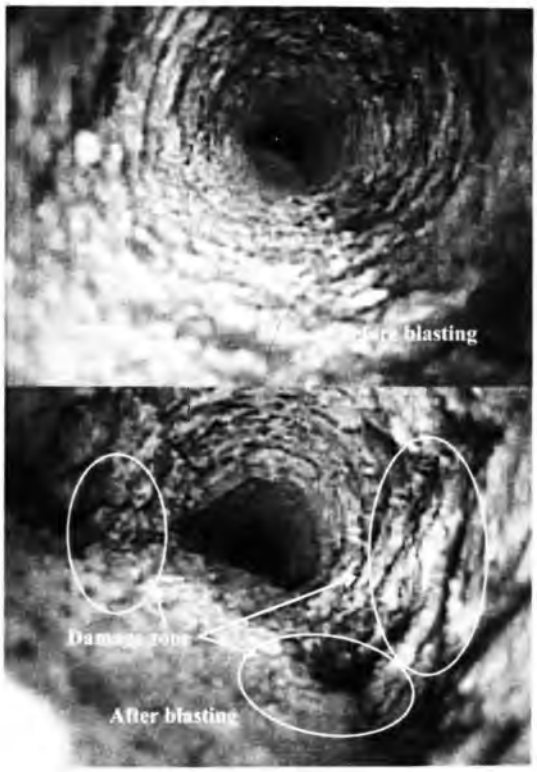

Figure 10. Images of pre-blast and post-blast inspection surveys of rock mass with acute joint orientations captured by borehole camera

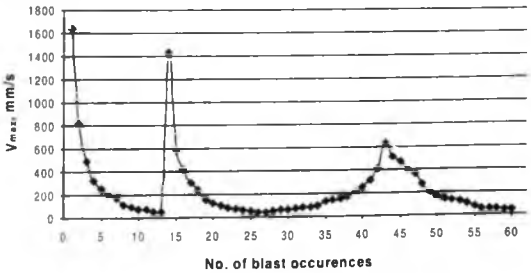

Fig. 11: Peak particle velocities versus no. of occurrences of dynamic loading in gneiss rock mass with obtuse joint orientation

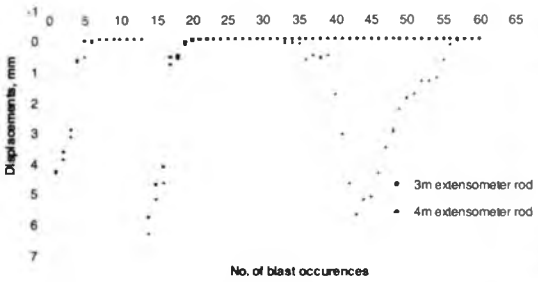

Fig. 12: Plastic deformations of extensometer rods in Gneiss rock mass with obtuse joint orientation

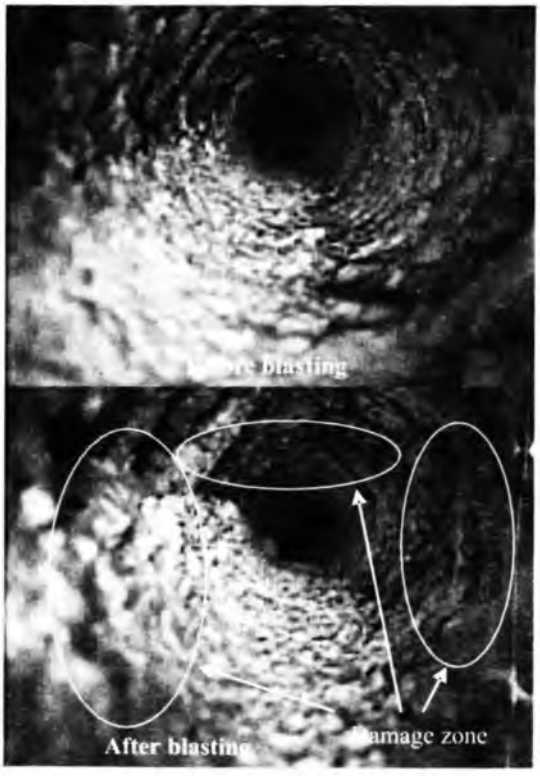

Fig. 13: Images of intact and disturbed rock mass with obtuse joint orientation, captured by borehole camera

field blast loadings. This might be the reason why the 3.0m extensometer rod did not respond to even the vibrations levels which were greater than the critical vibration levels. There were substantial displacements observed to the 4.0m extensometer rod (Fig. 12) for the V_{max} levels above V_{cr} for the MAT and CVT blast rounds and no displacements (>1mm) were observed for the V_{max} levels

Fig. 14: Roof failure due to extension of fractures on account of repeated blast induced damage

below V_{cr} for the blast rounds of same locations. After 40 rounds of blast occurrences, the displacements were again observed at the vibration level, 254 mm/s, which is much below the V_{cr}. There were no displacements observed below the V_{max} level (98 mm/s). This result gives an inference that the anchor point of 4.0m rod was in elastic zone and the damage zone was within 4m from the tunnel perimeter. The borehole inspection survey was conducted to cross check the damage assessment by extensometers and for exact damage measurement. The images of borehole sections which contain the interface of intact and disturbed rock mass are shown in Fig. 13. The maximum damage depth measured by the borehole camera survey with obtuse joint angle orientation was 3.6m. This was the reason for the roof failure that occurred near the test site. The roof failure due to extension of fractures beyond 3m due to repeated blast induced damage is shown in Fig. 14. The maximum length of roof bolts designed for that rock mass was also 3m.

Results

The near field blast loading due to main tunnel excavations, could generate displacements in the rock mass, only when the peak particle velocity exceeded the critical vibration levels (V_{cr}). After repeated exposures of vibrations due to blast rounds at MAT, CVT and TRT, plastic displacements observed even at lower levels of vibrations than the V_{cr}. The extra

damage due to repeated blast loading was 1.11m and 1.86m at the left-side and right-side walls of the tunnel respectively.

After the occurrences of 53 numbers of blast rounds with the V_{max} levels ranging from 40-1753 mm/s, considerable displacements observed in the extensometer even at the V_{max} level of 116 mm/s, which is approximately 33% of V_{cr} in the Gneiss rock mass with acute joint orientation. The displacements observed at the V_{max} level of 98 mm/s i.e. at approximately 23% of V_{cr} in the gneiss rock mass with obtuse joint orientation, after 54 numbers of occurrences of blast loading. These results are well in line with the observations of Dowding & Rosen (1978). The threshold vibration limits with number of cycles of repeated loading for two different rock masses are given in Table 4. The study also reveals that the overall damage was about 33% more at right-side rock mass, in comparison to the left-side rock mass. The observations also indicate that the repeated dynamic loading resulted in the damage at the vibration levels even at 23 % of V_{cr} when the unfavorable joints exist. These observations were almost similar to the findings of Adamson and Scherpenisse (1998), which says that threshold vibration level falls down to 25% of V_{cr} in repeated loading conditions. The findings of the study clearly indicate that the phenomena of repeated blasting with respect to number of cycles of loading should be taken in to consideration for proper assessment of comprehensive blast induced damage.

Conclusions

A comprehensive blast monitoring program aimed at the investigation on the effect of repeated blast induced damage due to near-field and far-field vibrations was conducted in gneiss rock mass. The damage levels predicted for near-field blast loading by Holmberg-Persson model were 1.40m and 1.30m for the left-side and right-side rock mass respectively. The damage levels measured for the same rock mass by borehole camera was 1.59m, and 1.74m for the left-side and right-side rock mass, respectively. Estimates of the maximum extent of rock mass damage made through the application of the Holmberg-Persson model compared well with measured results for left-side wall, although the former one was at lower side of damage. The damage results of Holmberg-Persson model deviated from the measured results for right-side wall. This might be because of the additional effect of joint orientations, playing a dominant role at right-side wall rock mass. Although there are deviations, the modelling approaches like Holmberg-Persson model are very useful for the project engineers for preliminary assessment and estimation of the damage and for practical methods to model peak particle velocity attenuation.

The study also found that repeated dynamic loading imparted on the exposed tunnel by subsequent blasts in the vicinity is going to contribute to rock mass weakening and preconditioning. After 53 repeated blast rounds, the threshold vibration level for the gneiss at left-side wall was found to be 116 mm/s. The dynamic loading due to repeated blasts resulted in 70% and 107% extra damage, in addition to the near-field damage, at left-side and right-side rock mass, respectively. The repeated dynamic loading also resulted in reduced threshold peak

Table 4: Far-field damage due to repeated loading at both the sides of tunnel wall

Location	Rock type	No of cycles of blast loading	Threshold vibration limits (mm/s)	Maximum Extent of damage (m)
Right-side wall (Joint orientation=150^0)	Schistose/Augan gneiss with obtuse joint orientation	53	116	2.70
Left-side wall (Joint orientation=30^0)	Schistose/Augan gneiss with acute joint orientation	52	98	3.60

particle velocity to 33% and 23% of critical peak particle velocity at left-side and right-side, respectively. The study also revealed that the overall damage was about 75% more at tunnel wall with obtuse angle joint orientation in comparison to the acute angle joint orientation. The findings of the study clearly indicate that the repeated blast loading extends damage to a substantially dangerous levels and the effect is severe in case of unfavorable joint orientations. Therefore the phenomena of repeated blasting with respect to number of cycles of loading is an important aspect to be considered for proper assessment of blast induced damage and for planning of safety measures of underground openings.

Acknowledgments

The authors express their sincere thanks to the Director, CIMFR (CMRI) for permitting to publish this paper. The authors also express their sincere thanks to all the scientists of CIMFR regional centre, Nagpur for their valuable assistance during the field work. The authors extend their thanks to the executives of M/s Patel Engineering Ltd. and NTPC for their cooperation during the field studies.

References

Andrieux, P., McKenzie, C., Heilig, J. and Drolet, A. (1994): The Impact of Blasting on Excavation Design – A Geomechanics Approach. *In: Proceedings of the 20th Symposium on Explosives and Blasting Research,* ISEE, January 30 - February 3, Austin, USA:107–119.

Atchison, T. C. and Pugliese, J.M. (1964): Comparative Studies of Explosives in Limestone. BuMines Rept. of Inv. 6395: 25.

Barton, N. and Hansteen, H. (1979): Very large span openings at shallow depth: deformation magnitudes from jointed models and finite element analysis. *In proc. 4th rapid Excavation & Tunneling conf.* (Atlanta), Vol.2: 1331-1353.

Beyer, R.R. and Jacobs, A.M. (1986): Borehole television for geotechnical investigations. *Water Power and Dam construction,* 38 (9): 16-28.

Brady, B.H. (1990): Dynamic performance and design of underground excavations in jointed rock. *Static and dynamic considerations of Rock Engineering,* Brummer (ed), Balkema, Rotterdam: 1-10.

Brown, E.T. and Hudson, J.A. (1974): Fatigue failure characteristics of some models of jointed rock. *Earthquake Engineering and structural dynamics,* 2: 379-386.

Chakraborty, A.K., Raina, A.K., Ramulu, M., Jethwa, J.L. & Gupta, R.N. (1998): Lake Tap at Koyna, *World Tunnel. Subsurface Exc.* November: 456-460.

Cunningham, C.V.B. and Goetzsche, A.F. (1996): The specification of blast damage limitations in tunneling contracts. *Tunneling and underground space technology* 5 (3): 23-27

Hendron, A.J. (1977): Engineering of Rock Blasting on Civil Projects. *Structural and Geotechnical Mechanics.* W.J. Hall (ed.), Prentice-Hall, Inc.

Holmberg, R. and Persson, P.A. (1980): Design of Tunnel Perimeter Blast Hole Patterns to Prevent Rock Damage. Trans. *Inst. Mining Metall.* 89: A37–A40.

Holmberg, R. (1993): Recent developments in control rock damage. *Rock Fragmentation by Blasting,* Rossamanith (ed.) A.A. Balkema, Rotterdam,Vienna, Austria, July 5-8: 197-198.

ISRM (1992): Commission on Testing methods, Suggested methods for installation of borehole extensometer, *International Society for Rock Mechanics.*

Jaeger, J.C. and Cook, N.G.W. (1979): Fundamentals of rock mechanics, 3rd ed. Chapman & Hall, London.

Langefors, U. and Kihlstrom, B. (1963): *The modern techniques of rock blasting.* New York: J. Wiley and Sons, Inc.

Law, T.M., May, J., Spathis, A.T., Du Plessis, A.T. and Palmer, A.M. (2001): Blast damage and blast dilution control: The application of bulk emulsion systems at the WMC St Ives junction mine, *Fragblast,* Vol. 5, No. 1-2, pp. 1-20

Lewandowski, T., Luan Mai, V.K. and Danell, R. (1996): Influence of discontinuities on presplitting effectiveness, *In: Proceedings of 5th Int. Symposium on Rock Fragmentation by Blasting,* Montrial, Canada, August: 217-225

Oriard, L.L. (1982): Blasting effects and their control, Underground Mining Methods Handbook, SME of AIME, Littleton, Colorado: 1590-1603.

Ramulu, M., Chakraborty, A. K. and Sitharam, T.G. (2009): Damage assessment of basaltic rock mass due to repeated blasting in a railway tunnelling project – a case study, *Tunneling and underground space technology,* Vol. 24: 208–221

Rocque, P. (1992): *Techniques utilized for the detection and characterization of blast induced damage.* M. Sc. Eng. Thesis, Queen's University at Kingston, Ontario, Canada, 251 p.

Singh, S.P. (1993): Damage causing potential of different explosives, Proc, *9th annual symposium on Explosives and Blasting Research,* January 31- February 4, San Diego, California: 325-337.

Singh, S.P. and Xavier, P. (2005): Causes, impact and control of overbreak in underground excavations, *Tunneling and underground space technology* 20 (2005): 63-71

St. John, C.M. and Zahrah, T.F. (1987): A seismic design of underground structures. *Tunneling and underground space Technology,* 2(2): 165-197.

Stacey, T.R., Cameron-Clarke and Mival, K. (1990): Stabilisation of old workings by blasting: Case study of a failed experiment, *Static and dynamic considerations of Rock Engineering,* Brummer (ed), Balkema, Rotterdam: 317-324.

Villaescusa, E., Onederra, I. and Scott, C. (2004): 'Blast Induced Damage and Dynamic Behaviour of Hanging walls in Bench Stoping', *Fragblast,* 8:1: 23 - 40

Wagner, H. (1984): Support requirements for rockburst conditions, *In Rockbursts and seismicity in mines,* S.Africa Inst. Min.& Met., Johannesbug: 209-218.